Sánchez Díaz, C.; Monrabal, J.; Gonzalez, D.; Alfonso Solar, D.; Peñalvo López, E. (2015). Experimental results of the hydrogen productioncontrol of a hydrogen energy buffer. International Journal of Hydrogen Energy. 40(15):5013-5024. doi:10.1016/j.ijhydene.2015.02.048.

Experimental results of the hydrogen production control of a hydrogen energy buffer.

Carlos Sánchez-Diaz, Javier Monrabal, Domingo González, David Alfonso, Elisa Peñalvo-López

Institute for Energy Engineering, Universitat Politècnica de València, Camino de Vera s/n, 46022 Valencia, Spain

csanched@eln.upv.es; dgn@iicv.es; daalso@die.upv.es; elpealpe@upvnet.upv.es

Corresponding author:

Carlos Sánchez

Phone Number: +34 653 953 003

Fax Number: +34 963 877 609

Email: csanched@eln.upv.es

Postal Address: Instituto de Ingeniería Energética, Universidad Politécnica de Valencia, Camino de Vera s/n, 46022, Valencia, Spain.

Abstract

High penetration of renewable energy requires high reliability to compensate the intermittency of the sources, which is generally tackled by using energy storage systems. However, the selection of the storage technology is not an easy task; it depends on parameters like efficiency, self-discharge, investment costs, etc. Among the different alternatives, hydrogen storage systems present several advantages, such as its low investment costs and inexistent self-discharge, but comparatively, it presents low efficiency. This paper introduces the experimental results of controlling a hydrogen storage system connected to a micro-grid based on renewable generation. The research has been carried out in LabDER at the Universitat Politècnica de València, a controlled laboratory designed for the study of distributed energy resources. During the research, a specific control system has been designed and assembled to regulate the hydrogen production , consuming just the excess of energy produced by the renewable sources. The paper includes the design process of the controller, including the experimental characterization of the elements and the experimental results of such control.

Keywords

Hybrid system; Renewable energy; Energy Storage; Experimental Control; Grid connected;

1. Introduction

Conventional energy resources are limited and scarce, rising energy prices and harmful emissions produced by fossil fuels. Power generation from conventional energy sources are unsustainable and, in many cases, economically unviable. Renewable energy resources have a high potential to alleviate this situation. However, increasing electricity contribution from these sources may cause low reliability of the electricity supply if it is not well designed, controlled and maintained.

Solar and wind energy are the most preferred renewable energy sources for their distributed availability [1], but its intermittency and unpredictability presents an important challenge when reliable energy is required. [2]. This intermittency may be alleviated integrating different renewable sources in hybrid systems but guaranteeing energy supply can only be achieved using energy storage systems [3]. There are many different available technologies for electricity storage (flywheels, batteries, compressed air, hydrogen…). Identifying the most adequate for each application involves identifying the needs and analyzing the parameters associated to the operative, besides the economics and sustainable aspects of them. Main considered parameters include the overall efficiency of the system, the self-discharging rate or the investment cost [4],[5]. Superconducting magnetic energy storages (SMES) present an efficiency of 95%, but are expensive and their energy rate is very small (approximately 10-15% of self-discharging). Flow batteries (FB) may storage large amounts of energy at an acceptable efficiency (65-87%), their self-discharge is nearly zero but investment cost are also high (500-600$/kWh) . In contrast, other technologies like flywheels provide high self-discharge (100%) or require geological structures, as it is the case of compressed air energy storage (CAES). In the case of hydrogen energy storage (HESS), despite efficiency is very low (35-42.5%), presents several advantages: self-discharge is zero and investment costs are very low (2-15 €/kWh), though.

This paper focuses on hydrogen storage as a promising solution since it can be easily stored also for long term applications and may be used in vehicles [6]. Among the different hydrogen generation technologies, which focus on electrolysis technologies for medium/large scale applications (10-360 Nm3/h of hydrogen production capacity, input power of electrolyzer in the range 50 – 2000 kW), alkaline water electrolysis is an economic, commercially available and mature technology [7, 8, 9] with many real cases operating nowadays. According to different manufacturers, alkaline electrolyzers operate at temperatures in the range of 70 – 140 ºC and pressures of 1 to 200 bar (usually lower than 30 bar) [10, 7]. These electrolyzers can reach efficiencies in the range of 60% to71% (HHV) [9]. Regarding hydrogen storage, the majority of electrolysis projects based on renewable energies (about 88%) use gas compression for hydrogen storage (pressures in the range 200 – 300 bar) due to the technology matureness, cost, and commercial availability of components. Only few projects implement other technologies (i.e. metal hydride) [7].

Hydrogen energy storage is specially indicated for micro-grid systems [11]. Previous simulation studies in this area [13, 14, 15] show that energy can be generated and stored near the consumptions points, increasing the reliability of the overall system and reducing the losses produced by large power lines [12].

The research presented in this paper has been carried out at LabDER, the distributed energy resources laboratory at Universitat Politècnica de València (Spain). The laboratory includes a micro-grid with a wind, a photovoltaic and a biomass gasifier system, together with hydrogen production. All systems are connected to the AC micro-grid using Acid-Pb batteries for immediate energy storage. Research studies in hydrogen production systems present its high complexity for modeling and control/ communication purposes [16, 17, 18] due to the energy consumption of auxiliary units, which are usually underestimated [19]. Energy consumption prediction of the whole system becomes difficult, thus power management strategies based on these systems require a control algorithm based on accurate and/or experimentally validated models. Main objective of this paper is to provide an experimentally validated methodology for accurate control algorithm design of a hydrogen generation and storage system, based on alkaline elecrolyzer and high pressure storage. This design methodology has been applied to a real system, obtaining a control algorithm and promising fitting results. The paper is structured as follows: Section 2 presents the description of the hydrogen production and storage system (including control and communications). Section 3 describes the control algorithm design of single components and the whole system based on both experimental data and theoretical equations. Section 4 includes results and discussion of the control algorithm implementation and testing. Main conclusions are presented in Section 5

2. Description of the Hydrogen production system

Hydrogen is generated by means of an alkaline electrolyser using distilled and deionized water, producing in the process, hydrogen and oxygen. Oxygen will be used to enrich the efficiency of the syngas generated at the biomass power plant, while hydrogen is pipelined to the purifying system to increase its purity to 99.995% (required for a PEM fuel cell). This process uses commercial refrigeration and compressed air equipment (see Table 1).

The system is an industrial process designed to maximize the production of hydrogen. Initially, the design included an electro-pneumatic valve connected to the purifying system output to control the hydrogen generation and, also, the energy consumed by the electrolyzer. However, the experimental characterization of the system demonstrated that this valve did not work as expected when the pressure of the hydrogen bottle increased [20]. Thereby, the valve activity was reduced to a security task. Whether a problem occurs, the valve closes, cutting the hydrogen flow.

Generated hydrogen is stored in a 50 liter gas bottle with a maximum pressure of 200 bar. Outlet pressure from the electrolyzer is 4 bars, therefore an additional booster to store the hydrogen at this pressure is used. This compressor operates with compressed air to avoid hydrogen contamination (i.e. oil in conventional compressors). Then, booster increases hydrogen pressure, as required, and sets the hydrogen flow demanded by the electrolyzer. Control design includes the booster as hydrogen flow control, which regulates the system by a Programmable Logic Device (PLC) and reads the data from a power monitoring device installed at the electrical connection of the hydrogen generator. This device can be easily accessed throughout a TCP/IP network and it provides information about the energy consumed by the system. PLC also reads data from the electrolyzer by means of an own designed gateway that connects it with the electrolyzer control system. Finally, an inductive sensor provides the swab speed to act over the pressure regulator in the compressed air. Figure 1 shows a block diagram of the complete hydrogen generation system and figure 2 shows a simplified block diagram of the control system.

The electrolyzer G2.0 requires a three-phase electric supply with a nominal power of 7.2 kW. The nominal current is 14 A and, in these conditions, nominal hydrogen production is 1.33 Nm^3/h at 2.5 bar of outlet pressure. Electrolyzer auxiliary systems represent a constant power of 500 W while generated hydrogen purity is between 99.3 and 99.8 %. In the designed system, outlet pressure is set to 4 bar, maximum water consumption is 1.2 l/h, and the electrolysis medium is a sodium hydroxide (NaOH) solution with 1.2 g/ml density. The entire electrolysis process is controlled by an ABB 07KT97 PLC. This device is connected to the tactile screen that serves as the interface with the user, and provides information about the energy consumed, hydrogen and oxygen flow, electrolysis cell current, pressure, temperature and other information related to the process. In addition, this PLC has a serial port capable to monitor all these parameters from an external device via a RS232 serial communication with Modbus RTU protocol.

Once hydrogen is produced, it is purified to extract residual oxygen, humidity and electrolytic solution from the hydrogen flow. The purifying system is based on a Pressure Swing Adsorption (PSA) process, which consists on a three filters (activated carbon, aluminum oxide and hygroscopic salts) and requires a minimum of 6 bar of compressed air flow supplied by the compressor. Nominal capacity of the purifying system is 6 Nm^3/h, higher than the electrolyzer capacity due to unavailability of such systems at kW scale. At the end, input hydrogen purity is more than 99% while output purity is 99.995%. Regarding the water steam, it is eliminated by condensation. This process is carried out by two heat exchangers, one internal with an air radiator and another one external with a nominal frigorific power of 3460 W. Figure 3 shows the electrolyzer and the purifying system.

The compressor has a 4 kW electric motor and can suction a nominal air flow of 700 liters per minute at 7 bars. Moreover, the tank has 300 liters of capacity and an operationrange of 6.5 -9 bars. Compressed air is used in the purifying system as well as in the electro-pneumatic valve and the booster. The electro-pneumatic valve is controlled by a 4 – 20 mA signal and constant air pressure of 6 bars, allowing the movement of the piston rod. A Phoenix Contact MCR-SL-U-I-4 module enables the transformation of a variable voltage between 0 to 10 V into a 4 – 20 mA signal. The booster uses the variable compressed air pressure to compress hydrogen, depending on the inlet hydrogen pressure and the bottle hydrogen pressure.

The Booster is a two-stage compressor that compresses hydrogen up to a maximum pressure of 200 bars. It is composed of an air section with a central pneumatic cylinder and a gas division with two compression cylinders, the first one with a compression ratio of 1:7 and the second one with a compression ratio of 1:30. Refrigeration of the compressor is carried out using the exhaust air of a heat exchanger, so no electrical supply is required. Pressure in the outlet pipeline is related to the hydrogen inlet pressure and compressed air pressure, since the outlet hydrogen pressure depends on the diameter relation between air cylinder and the corresponding hydrogen cylinder in each stage. Figure 4 shows a scheme including the two phases: suction and compression, where hydrogen is suctioned from the inlet pipeline and compressed at a high pressure in the outlet pipeline.

Output pressure depends on the relationship between the two pistons' section (air and output hydrogen) and the difference between air pressure and output pressure. The second stage transfers hydrogen from the intermediate pressure to the high pressure hydrogen cylinder. The mathematical relation between the different pressures, hydrogen inlet, compressed air pressure and hydrogen cylinder, is presented in equation 1.

$$P_o = 30 \cdot P_{ab} + 4.2 \cdot P_s \tag{1}$$

where P_o is output hydrogen pressure, P_{ab} is compressed air pressure, and P_s is hydrogen supply pressure. Among these parameters, just the compressed air pressure is independent and may be modified using a commanded pressure regulator which is controlled by the ILC 150 PLC.

The hydrogen flow, compressed by the booster, is a function of the air flow. It determines the number of piston cycles and the volumetric efficiency, which depends on the bottle pressure. Hydrogen flow through gas booster is calculated by equation 2.

$$Q_{H2} = \frac{\frac{V_p}{V_{p(\max)}} \cdot V_e \cdot D_b \cdot (P_s + 1.013)}{1.013} \tag{2}$$

where Q_{H2} is hydrogen flow, V_p is the number of piston cycles per minute, $V_{p(\max)}$ is the maximum piston cycles with null output pressure, V_e is the volumetric efficiency, D_b is geometrical volume of gas piston and P_s is hydrogen supply pressure. Once again, the independent parameter is the air pressure related to the air flow. Thus, there is a relationship between output hydrogen pressure and hydrogen flow.

The control algorithm, described in the next section, runs in a Phoenix Contact ILC 150 ETH PLC. The device has an Ethernet connection to communicate with other devices using Modbus as the communication protocol. There are two main versions of this protocol: TCP/IP (which runs over an Ethernet network) and RTU (which runs over a serial network, RS232 or RS485, depending on the physical layer implemented). Modbus is based on a Client/Server architecture (also known as Master/Slave).

Server (or Slave) is always on stand-by mode, waiting for the Client request (Master). The ILC 150 PLC is connected to a standard switch with Ethernet cable and defines the physical network. The other elements of the system are also connected using the same Ethernet network, such as the grid analyzer which is accessible by means of Modbus protocol. Contrariwise, the ABB PLC integrated in the Electrolyzer, which acts as a slave, uses Modbus RTU protocol by means of a RS-232 port. Thus, it cannot be directly integrated into the Ethernet network. Consequently, a gateway was built and programmed to translate data from Modbus RTU to Modbus TCP/IP. Figure 5 shows a picture of the gateway and how it is connected within the electrolyzer.

Electrical power consumption by the electrolyzer is recorded by SENTRON and parameters like cell current, cell temperature, hydrogen and oxygen flow, as well as other additional information is provided by the ABB PLC. The control system also records the speed of the booster piston cycle. This is obtained by an inductive sensor located next to the displaced rod when internal pneumatic valve is activated at each booster cycle.

As previously stated, electrical power depends on the produced hydrogen flow, which is directly related to the speed of the booster piston cycle. Controlling hydrogen production implies regulating the air pressure. This task is carried out by a Festo VVPM pressure regulator, commanded by a 0-10 V signal coming from the analog output in the IL AO 2/U/BP-PAC module of the ILC150 PLC.

A Modbus Server was developed in the ILC 150 PLC to contain all the necessary data for implementing the system control. Furthermore, an acquisition software was also developed using Python language [21] running over a Linux platform to access as Modbus Client to this server. This data acquisition software is structured in two main modules. The first one initiates the communication with the corresponding system and records the data (called SAD module), while the second one generates the graphical user interface (called PLOT module).

In addition, the user may run a supplementary module, named MARK. This extra module allows the user to define temporary tags during the experimental tests. The tags identify the time when a significant event happens during the test and record these data in the SAD module with the rest of the collected information. During the experiment, the procedure is always the same. First the hydrogen generation system starts (including control system) and then, the SAD and MARK modules commence running. The test continues by introducing the pre-defined modifications in the parameters as planned in the experimental design. Finally, once the experiment is over, both software modules close and PLOT module starts, representing a set of graphs including user marks (see Results section).

3. Control algorithm design procedure

In a previous paper, the corresponding author presented the initial experimental characterization of the whole system [20], including a specific control algorithm. Actual control algorithm builds from previous one but introducing significant improvements in evaluating the “energy consumed” and the “equivalent production of hydrogen”, since it has been demonstrated that not all energy consumed by the electrolyzer is used to produce hydrogen. Intermediate calculations have been introduced in the model in order to consider the energy consumed in other uses such as auxiliary systems´ supply (cooling systems, i.e.) or dissipated heat. Experimental analysis of these data showed that energy consumed by other uses can be easily predicted since it is approximately constant.

Figure 6 shows a block diagram of the algorithm. The energy surplus generated by the renewable hybrid system at LabDER is used to produce hydrogen. In these cases, central control of the micro-grid sends the energy excess command to the hydrogen control system by means the Ethernet connection (E_{exc}). At this point, the electrolysis cell current corresponding to this energy excess is calculated (I_C) together with its equivalent hydrogen flow (Q_{H2}). Then, it is determined the required speed of the booster swabbing (V_p) and booster air drive pressure. In order to define the required booster air drive pressure (P_{ab}), a hydrogen storage pressure (P_b) is considered and a control of the voltage is implemented in the air pressure regulator ($V_{control}$). Finally, from the stationary assessment, the PID controlled is designed and implemented to analyze the dynamic behavior of the system. Next, it is described each of the calculations.

Cell Current from Active Power. The electrolyzer is connected to the three-phase grid. DC current in the electrolysis cell arrives through a fully controlled three-phase rectifier connected to a large inductance, which filters the harmonic components of the current. Active power consumed at the rectifier input is approximately the same as in the electrolyzer cell, therefore rectifier power losses are considered negligible. It is used active power instead of apparent since its behavior adjusts better in open loop, as it was revealed in the tests carried out in the experimental characterization. Figure 7 shows the relationship between active power consumed by the rectifier input and the cell current. From this figure, best curve fitting was expressed in equation 3, showing a relationship of 99% adjustment.

$$I_C = -2.617 + 7.418 \cdot 10^{-3} \cdot P_{Act} \tag{3}$$

where I_C is the cell current and P_{Act} is the active power.

Hydrogen Flow from Cell Current. Number of moles produced by the current could be calculated following the expression given in equation 4.

$$n_{H_2} = \frac{n_F \cdot n_C \cdot I_C}{z \cdot F} \tag{4}$$

where n_{H2} is the number of hydrogen moles, n_F is the Faraday efficiency, n_c is the number of electrolysis cells, I_C is the cell current, z is the number of electrons from hydrogen and F is the Faraday constant.

Considering all these parameters constant, produced hydrogen is expected to be linear with respect to current, however experimental tests indicate slightly different results. Figure 8 represents the relationship between cell current and hydrogen flow produced by the electrolyzer. As it may be observed, below a current of 39 A, experimental data is not linear, therefore an additional curve fitting is required. Equation 5 represents this fitting with 99% of accuracy.

$$\begin{aligned} Q_{H_2} = {} & 1.389 \cdot 10^{-3} + 1.111 \cdot 10^{-2} \cdot I_C - 6.302 \cdot 10^{-4} \cdot {I_C}^2 + 3.959 \cdot 10^{-5} \cdot {I_C}^3 \\ & - 4.417 \cdot 10^{-7} \cdot {I_C}^4 \end{aligned} \tag{5}$$

where Q_{H2} is the hydrogen flow in Nm^3/h.

Swabbing speed from hydrogen flow. The relationship between these two variables is just geometric. Booster inlet piston has a particular capacity when the piston is in the right position (figure 4). The faster the piston moves, the more hydrogen is displaced per time unit. Equation 2 allows calculating the number of piston cycles per minute, considering that volumetric efficiency (V_e) depends on the hydrogen output pressure (storage bottle pressure) as it is given by equation 6.

$$V_e = 1.04 - \frac{0.01 \cdot P_O + 1.013}{P_S + 1.013} \tag{6}$$

where P_o is the booster output pressure and P_S is the hydrogen supply (input) pressure.

Driving air pressure from swabbing speed. This is the most challenging variable to calculate. Figure 4 shows a simplified diagram of the booster behavior in two stages. Pressure supplied by the hydrogen line is considered constant in the analysis and equal to 4 bars. In these conditions, compressed air entering the central cavity displaces the piston to the right position if there is enough air pressure provided by the hydrogen bottle pressure (considering the relationship between piston sections in the air cavity and second stage of gas cavity).

Piston movement introduces initial hydrogen in the first stage of the gas cavity, whereas in the second stage of the compression work, compressed air enters the right air cavity, displacing the piston to the left and compressing hydrogen to an intermediate pressure. In the second gas cavity, the piston´s displacement causes a suction effect and the piston movement compresses the hydrogen until bottle pressure is reached. Relationship between air pressure, hydrogen inlet pressure and hydrogen output pressure (bottle pressure) determines the movement of the piston (if there is enough air pressure) and speed of each cycle. Once equilibrium is reached, excess of air pressure is used to generate the force moving the piston and its speed. Figure 9 shows the booster operation limits, considering air pressure and bottle pressure.

An exact dynamic model of the booster is very complicated to define since pressure at each hydrogen cavity changes as the piston is moving [22]. For this reason, an approximated model is considered. Figure 10 shows the balanced force at each stage of operation. In the model, the dynamic behavior is expressed according to equation 7, where friction forces are not considered. Equation 7.a corresponds to situation a) in figure 10 while equation 7.b represents situation b) in figure 10.

$$\sum_{i=1}^{n} F_i = P_{c1} \cdot S_1 + P_{ab} \cdot S' - P_{at} \cdot S' - P_{c2} \cdot S_2 = M \frac{d^2x}{dt^2} \qquad (7.a)$$

$$\sum_{i=1}^{n} F_i = P_{c1} \cdot S_2 + P_{ab} \cdot S' - P_{at} \cdot S' - P_{c1} \cdot S_1 = M \frac{d^2x}{dt^2} \qquad (7.b)$$

where P_{ab} is the driving air pressure, P_{c1} is the cavity 1 pressure, P_{c2} is cavity 2 pressure, S_1 is the piston section of cavity 1, S_2 is the piston section of cavity 2, S’ is the piston section of air cavity (deducting central axis section), M is the mass of piston and x is the displacement of piston.

The model for the piston behavior is obtained solving these equations and, therefore, the booster swabbing speed. The relation between the piston movement and pressures has been approached through experimental approximation, using several bottle pressures (in steps of 1 bar) and different driving air pressure, thereby obtaining the piston cycling speed. This empiric method provides a set of values for each of the 200 bottle pressures, since the bottle reaches 200 bars. Then, a polynomial fitting is applied obtaining a family of curved functions. Figure 11 shows these functions in 5 bars steps in order to make it clearer for the reader. Control algorithm uses the complete family functions built with 1 bar steps. Obtained air pressure is supplied by the air pressure regulator VVPM. Maximum pressure required is 6 bars and the regulator provides it proportionally from 0 to 10 bars. Control input is a 0 – 10 V, which is given by the ILC analog output.

PID regulator. Once the production of hydrogen can be modified using an analog output from the ILC, the dynamic response of the system is analyzed. The objective is to design and develop a PID controller capable to maintain the power consumption in the value determined by the central control, which is related to the energy´s excess. Complexity of the system made very difficult to obtain an analytical expression for this dynamic behavior. Thus, an identification method is used, which consist on applying a known control step and then, analyzing the system´s response of the open loop. This system behavior is identified as a known system response (first or second order). Figure

12 shows the response of the open loop system and modelled system response developed as a first order system with a finite delay. Constant time of the system is 63 seconds and delay is 23 seconds.

Once system response is known, values of time constants in the PID controller are obtained using the well-known Ziegler-Nichols method. Equation 8 shows the general expression for a PID controller [23].

$$u(t) = K_p \left[e(t) + \frac{1}{T_i} \int_{-\infty}^{t} e(t)dt + T_d \frac{de(t)}{dt} \right] \tag{8}$$

where u(t) is the control action and e(t) is the error, the difference between command power and power consumed by the electrolyzer. K_p is the proportional constant, T_i is the integral time constant and T_d is the derivative time constant.

Equation 9 shows the PID function transfer using Laplace Transform.

$$G(s) = K_p + \frac{K_i}{s} + K_d s \tag{9}$$

where G(s) is the relation between u(s) and e(s), K_i includes K_p and T_i and K_d includes K_p and T_d.

In this case, it is used the tuning option provided by Matlab PID block, which analyzes the system´s test facility and optimizes the control parameters for a required response. Using this method, constants of the PID are the following

$K_p = 0.9477$; $K_i = 0.0204$; $K_d = 0$

This corresponds to a PI controller. Using the digital system to control the test facility, the continuous regulator must be converted to discrete, thereby the well-known bi-lineal transform is used [24]. As a result, PID transfer function obtained is shown in equation 10

$$G(z) = \frac{u_k}{e_k} = \frac{k_1 + k_2 \cdot z^{-1} + k_3 \cdot z^{-2}}{1 - z^{-1}} \tag{10}$$

where u_k is the discrete control action, e_k is the discrete error signal and constants are calculated using the following equivalences:

$$\begin{gathered} k_1 = K_p + \frac{K_p}{T} + K_i \cdot T \\ k_2 = K_i \cdot T - \frac{2 \cdot K_d}{T} \\ k_3 = \frac{K_d}{T - K_p} \end{gathered} \tag{11}$$

where T is the sampling period, the time between a power consumed reading and the next sampling period. Taking into account the system constant time (63 seconds) and considering that the digital system completes a reading sequence in 100 ms, the sample period selected is 2 seconds.

Equation 10 can be expressed considering the term z^{-1} as the previous sample period and z^{-2} referring to the preceding previous sample period. Taking this into account, equation is calculated as showed in equation 12.

$$u_k = u_{k-1} + k_1 \cdot e_k + k_2 \cdot e_{k-1} + k_3 \cdot e_{k-2} \tag{12}$$

where k, k-1 and k-2 subscripts are referring to current sample period, previous sample period and preceding previous sample period, respectively. Appendix A shows the PLC source code that implements this equation.

4. Results and discussion

Complete algorithm presented in this paper was programmed in ILC 150 PLC, which acts as a control node of the hydrogen production and storage. PLC is connected to an Ethernet grid, as it is described in previous sections, which allows connecting it to the central control of the micro-grid in order to receive the power command.

During the investigation, a central control simulator was built in order to carry out several experimental tests. The simulator acts as the central control of the micro-grid, sending the initial command to the electrolyzer, indicating the power to be consumed. Using the central control simulator allows programming different command power curves and analyzing the response of the system. Figure 13 shows this response when the command power demanded is 5500W at 50 seconds, 4500W at 1200 seconds, 6500W at 1400 seconds and 6000W at 1700 seconds. As it may be observed in the figure, blue dots represent real consumed power while red line represents the PID controller output. Initially, in the first power change at 50 seconds, the limit imposed acted out since the calculated control action was more than 9000W. Then, power consumed was increased, obtaining an expected behavior of the system, considering its constant time. Overshoot was 12%, less than the 20% designed. However, at 200 seconds, a sudden increase of the consumed power occurred. Controller tried to compensate it, but at 400 seconds the behavior repeats. Afterwards, this situation was reproduced four times more. Increasing power represents less than 20% of the demanded power and the duration of the events varies, with a maximum of 250 seconds.

This behavior may be due to several causes. Main one is the electrolyzer algorithm of operation. Consumed power depends on the pressure of intermediate tanks. If there is a pressure down in the hydrogen intermediate tank, the control of the electrolyzer increases the electrolytic cell current in order to increase hydrogen production and, consequently, increase the tank pressure. This pressure fall is due to the behavior of the hydrogen purifying system. Hydrogen consumed by this element is not constant and causes this situation. In order to prevent these power excursions, a new PID was designed, introducing a derivative effect which could achieve a faster response to these power variations. Using the same procedure that in the previous one, rise time was increased to 36 seconds and constants values were the following:

$$K_p=1.6028 \quad ; \quad K_i=0.0163 \quad ; \quad K_d=3.2389$$

Figure 14 shows the command power change, consumed power and PID control action. It can be seen in 300 seconds how the pressurization process starts. In 620 seconds, a step of 5500 W is applied in the power command. Due to the effect of derivative action, oscillations caused by the depurator behavior increased, making the system more unstable.

Although maximum power variations suppose just the 27% of command power and its duration is very limited (minimizing its effect if hourly energy is considered), possible solutions were investigated. As the problem comes from the purifying system behavior, a possible solution would be the connection of a small intermediate hydrogen storage between the electrolyzer and purifying system. This storage would act as a lung which could smooth the variations out.

Another possible cause to this behavior is the control algorithm action when booster driving air is calculated using the family curves. Figure 15 shows the system behavior of experiment showed in figure 13 and the curve number used. It is possible that curve used was not the most adequate for calculating it. A more accurate process for curve selection should be carried out and checked.

5. Conclusion

In this paper, the hydrogen production system installed at LabDER laboratory, as part of the hydrogen energy storage system, is described. Hydrogen production is connected to a micro-grid together with other renewable energy sources (solar photovoltaic, wind energy and biomass gasification power plant). During the experimental research work, the excess of renewable energy production was directed to the production of hydrogen system and controlled to consume this excess of energy. A detailed description of each component behavior within the hydrogen production system was provided in order to complete the control algorithm design and provide an experimentally validated procedure. Equations describing the relationship between system variables are used to implement the digital calculations. Finally, dynamic response of the complete system is analyzed. Along the paper, a detailed description of the digital regulator design is made, designing the continuous proportional, integral and derivative (PID) regulator and, then, discretizing it. Results showed that the behavior of the overall system was acceptable, but some problems occurred. A non-periodic power consumption variation in the electrolyzer was detected. This variation is caused by the intrinsic behavior of the hydrogen purifying system combined with the control algorithm of the electrolyzer. Despite that maximum increments were of 27% of demanded power and duration was less than 250 seconds, modifications of hydrogen system and control system are suggested. In the hydrogen system, intermediate hydrogen storage between the electrolyzer and hydrogen purifying system could help to smooth the oscillations out. Furthermore, a more accurate process of pressure curve selection in the digital control algorithm could also help to increase the speed of the system´s response and compensate these variations.

Appendix A. Digital PID source code.

Following, it is showed the written PID source code which runs every time the period time is reached.

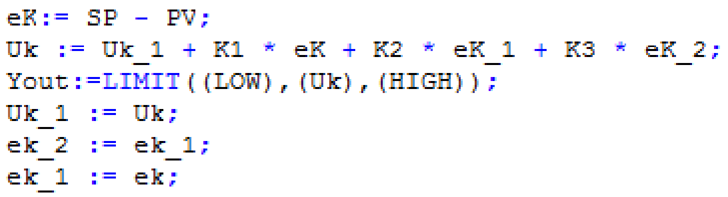

```
eK:= SP - PV;
Uk := Uk_1 + K1 * eK + K2 * eK_1 + K3 * eK_2;
Yout:=LIMIT((LOW),(Uk),(HIGH));
Uk_1 := Uk;
ek_2 := ek_1;
ek_1 := ek;
```

SP is the command power to be consumed and PV is the current power read from the Sentron device. After the new action control is calculated (Uk), all the registers are transferred to be prepared for the new sample period.

References

[1] Deshmukh MK, Deshmukh SS. Modeling of hybrid renewable energy systems. Renew Sustain Energy Rev 2008;12:235-49.

[2] H. Ibrahim, A. Ilinca, J. Perron, Energy storage systems—Characteristics and comparisons Renew Sustain Energy Rev 2008; 12: 1221-50.

[3] Paska Jozef, Biczel Piotr, K1os Mariusz. Hybrid power systems-an effective way of utilising primary energy sources. Renew Energy 2009; 34: 2414-21.

[4] Francisco Díaz-González, Andreas Sumper, Oriol Gomis-Bellmunt, Roberto Villafáfila-Robles. A review of energy storage technologies for wind power applications. Renew Sustain Energy Rev 2012; 16: 2154-71.

[5] Nor Shahida Hasan, Mohammad Yusri Hassan, Md Shah Majid, Hasimah Abdul Rahman. Review of storage schemes for wind energy systems. Renew Sustain Energy Rev 2013; 21: 237-47.

[6] Ernesto Amores, Jesús Rodríguez, Christian Carreras Influence of operation parameters in the modeling of alkaline water electrolyzers for hydrogen production, Int J Hydrogen Energy 2014; 39: 13063-78.

[7] Gerda Gahleitner, Hydrogen from renewable electricity: An international review of power-to-gas pilot plants for stationary applications. Int J Hydrogen Energy 2013, 38: 2039-61

[8] Mehmed Eroglu, Erkan Dursun, Suat Sevencan, Junseok Song, Suha Yazici, Osman Kilic. A mobile renewable house using PV/wind/fuel cell hybrid power system. Int J Hydrogen Energy 2011, 36: 7985-92

[9] Hollady JD, Hu J, King DL, Wang Y. An overview of hydrogen production technologies. Catalysis Today 2009;139:244-60

[10] Sterner M. Bioenergy and renewable power methane in integrated 100% renewable energy systems. Limiting global warming by transforming energy systems. Dissertation; 2009. <http://www.uni-kassel.de/upress/online/frei/978-3-89958-7982.volltext.frei.pdf>[accessed 30.07.14].

[11] H.M. Khodr, N.El Halabi, M. García-García. Intelligent renewable microgrid scheduling controlled by a virtual power producer: A laboratory experience. Renew Energy 2012; 48: 269-75.

[12] Guest editorial. Editorial special issue on power electronicsfor micrgrids – Part I. IEEE Tran Power Electronics, 2010; 25: 2885-8.

[13] Abdulkerim Karabiber, Cemal Keles, Asim Kaygusuz, B. Baykant Alagoz. An approach for the integration of renewable distributed generation in hybrid DC/AC microgrids. Renew Energy, 2013; 52: 251-59.

[14] Zacariah Iverson, Ajit Achutan, Pier Marzocca, Daryush Aidun. Optimal design of hybrid renewable energy system (HRES) using hydrogen storage technology for data center applications. Renew Energy, 2013; 52: 79-87.

[15] Omar Hafez, Kankar Bhattacharya. Optimal planning and design of a renewable energy system based supply system for microgrids. Renew Energy, 2012; 45: 7-15.

[16] Galli S. The solar-hydrogen SAPHYS project: operating results. Italy: ENEA, <http://gasunie.eldoc.ub.rug.nl/ FILES/root/1998/2044920/2044920.pdf>; 2003 [accessed 30.07.14].

[17] Chaparro AM, Soler J, Escudero MJ, de Ceballos EML, Wittstadt U, Daza L. Data results and operational experience with a solar hydrogen system. J Power Sources 2005;144:165-169.

[18] Correas L, Aso I. Task 24: wind energy and hydrogen integration, Proceedings of the 18th World Hydrogen Energy Conference, WHEC 2010, Essen, Germany, ISBN: 978-3-89336-654-5 (Parallel sessions book 4: Storage systems / policy perspectives)

[19] Szyszka A. Ten years of solar hydrogen demonstration project at Neunburg vorm Wald, Germany. Int J Hydrogen Energy 1998; 23: 849-60.

[20] Carlos Sánchez, Domingo González. Experimental Characterization of a grid-connected hydrogen energy buffer: Hydrogen production. Int J Hydrogen Energy 2013, 38: 9741-54

[21] B.G. Penaflor, J.R. Ferron, D.A. Piglowski, R.D. Johnson, M.L. Walker. Real-time data acquisition and feedback control using Linux Intel computers. Fusion Eng. and Des. 2006; 81: 1923-6.

[22] H. Wang, W. Xiong, and Z. Li. Dynamic simulation and experimental research on charge of gas booster. Proc of the 7th JFPS International Symposium on Fluid Power, TOYAMA 2008, 1-30.

[23] Katsuhiko Ogata. Modern control engineering. 2nd ed. London: Prentice Hall; 1993.

[24] Katsuhiko Ogata. Discrete time control systems. 2nd ed. London: Prentice Hall; 1996.